Utilizing OCT Nerve Fiber Layer and Ganglion Cell Layer Parameters to Predict Visual Field Severity in Glaucoma

Michael J. Cymbor, OD, FAAO[1]
Nittany Eye Associates, State College, PA
Adjunct Professor at Salus, Philadelphia, PA

Dustin E. Brown, OD
Nittany Eye Associates, State College, PA

Timothy Simin, Ph.D.
Penn State University, State College, PA

Abstract

Significance There currently exists no accepted optical coherence tomography severity staging system in glaucoma management. It is important to determine which optical coherence tomography metrics, or which combination of metrics, may best be used to predict visual field severity.

Purpose The purpose of this study is to evaluate different optical coherence tomography nerve fiber layer and ganglion cell complex parameters, specifically the focal loss volume percent and the global loss volume percent in different visual field groupings to determine which optical coherence tomography metrics are the most significant predictors of visual field defect severity.

Methods 186 eyes from 97 patients including 44 males and 53 females who were diagnosed with glaucoma were included in the study. Three anatomic regions were imaged including the optic disc, peripapillary nerve fiber layer, and the ganglion cell complex. Visual fields were graded using the Enhanced Glaucoma Staging System grading scale.

Results Focal loss volume produces the highest area under the curve of 0.79 as an individual predictor of being in the high-risk Enhanced Glaucoma Staging System group. The best liner multivariate model produced an area under the curve of 0.825. Applying a machine learning algorithm that combines variates and their interactions produces an area under the curve of 0.92.

Conclusions Focal loss volume and global loss volume and other optical coherence tomography parameters may be useful to incorporate into a multivariate model that also takes interactions into account to help clinicians determine the severity of their patient's glaucoma.

[1] Corresponding Author: Michael Cymbor, OD, FAAO, 177 Brothers Court, Port Matilda, PA 16870, mcymbor@nittanyeye.com

Glaucoma is a degenerative optic neuropathy characterized by a progressive loss of retinal ganglion cells, leading to a loss of visual function. Glaucoma is the second leading cause of blindness in the United States and the world.[1] From 2010 to 2050, the number of people in the U.S. with glaucoma is expected to more than double.[2] Vision loss in glaucoma is usually irreversible and progressive. As glaucoma becomes more common and life expectancy increases, the importance of understanding the disease increases.

Traditionally, glaucoma is functionally managed by visual fields. But visual fields have poor reproducibility and are subjective.[3] While the 24 degrees, second pattern visual field (24-2) or glaucoma tendency oriented perimetry (GTOP) pattern is most commonly used, the ten degrees, second pattern (10-2) also has value as some patients with glaucomatous optic neuropathy have undetected central defects when tested with a 24-2 pattern.[4] There are several methods for judging glaucoma severity based on visual fields including Hodapp-Anderson-Parrish (HAP), Glaucoma Staging System (GSS), Glaucoma Staging System 2 (GSS2) among others.[5,6] Newer software tools exist to help identify progression that are both event and trend-based. Event analysis may be more effective in early glaucoma as trend-based analyses in early glaucoma has been shown to have a ceiling effect.[7] Trend-based field analyses are more informative in moderate-to-severe glaucoma.[8] A weakness in visual field usage is that there is no gold standard for judging glaucomatous visual field severity.

Electrodiagnostic testing is another way to monitor visual function. The pattern electroretinogram (PERG) is an objective measurement of retinal ganglion cell function and is sensitive to glaucomatous damage.[9] Pattern electroretinograms may also show defects sooner

than traditional visual fields early in the disease state.[10] Unlike visual fields, pattern electroretinogram testing may show an improvement upon reducing intraocular pressure (IOP).[11]

Glaucoma has been structurally managed by comparing nerve photos.[12] This method is subjective, time consuming, and agreement is generally fair to poor.[13,14] There has been at least one software tool that simplified nerve photo comparison by “flickering” two images of the nerve and nerve fiber layer.[15] Confocal laser scanning tomography (HRT) and scanning laser polarimetry (GDx) simplified the detection of glaucomatous progression. Both technologies helped solidify the concept that structural change can precede visual field loss.[16,17] This principle became known as "preperimetric glaucoma".

Commercially available 1st generation optical coherence technology (OCT) (Stratus, Carl Zeiss, Dublin, CA) became available and many glaucoma clinicians embraced the technology. While it showed potential, it had numerous weaknesses including a slow scanning speed, limited resolution and inadequate reproducibility, along with lack of image registration.[18] All of those limitations have been improved with spectral domain optical coherence tomography.[19, 20]

Both time-domain and then fourier domain optical coherence tomography initially concentrated on the nerve fiber layer in glaucoma management. Retinal nerve fiber layer (RNFL) thinning is an independent predictor for glaucomatous visual field change.[21]

Since over 30% of retinal ganglion cells are found within the macular area, optical coherence tomography technology eventually focused on the macular area and found that macular scans are complementary to retinal nerve fiber layer scans.[22,23,24,25] Further research found that macular scans may even detect damage prior to retinal nerve fiber layer scans.[26,27] Optical

coherence tomography is considered to be more sensitive in the early stages of glaucoma than visual fields and may be less important in advanced glaucoma.[28] However, at least one study suggests that optical coherence tomography may be useful in advanced glaucoma.[29] Fourier domain optical coherence tomography can also detect glaucomatous progression.[30,31]

Currently, optical coherence tomography is arguably the most important instrument in managing glaucoma. One study claims that optical coherence tomography may be the best instrument necessary in the diagnosis of early glaucoma.[32] One weakness in using optical coherence tomography in the management of glaucoma is that there is no accepted standardization for grading glaucoma severity.

Glaucomatous optic neuropathy affects the nerves, nerve fiber layer and the ganglion cell complex (GCC) in similar patterns. The ganglion cell complex is defined as the nerve fiber layer, the ganglion cell layer, and the inner plexiform layer. The ganglion cell complex global loss volume (GLV) and focal loss volume (FLV) are pattern-based parameters.[33] Previous studies have shown that borderline or abnormal focal loss volume %'s increase the risk of glaucomatous conversion.[34]

Because of the many limitations of visual fields, structural tests that can more accurately determine risk for glaucoma conversion and progression are paramount.

The purpose of this study is to evaluate different optical coherence tomography nerve fiber layer and ganglion cell complex parameters, specifically the focal loss volume % and global loss volume % in different visual field groupings to determine which metrics are the most significant predictors of visual field defect severity using Enhanced Glaucoma Staging System (GSS2) grading.

Methods:

All data analyzed in this study come from patients at Nittany Eye Associates, State College, PA. The Institution Review Board (IRB) from Salus University (PA College of Optometry) approved the study protocol. The study agreed with the provisions of the Declaration of Helsinki. The study was in accordance with the Health Insurance Portability and Accountability Act of 1996 (HIPAA) privacy and security regulations.

Three anatomic regions were imaged including the optic disc, peripapillary nerve fiber layer, and the ganglion cell complex. The optical coherence tomography imaging device is the Avanti Widefield OCT (Optovue, Inc, Fremont, CA). The ganglion cell complex scan covered a 7x7mm square area in the macula. Scans were centered 1mm temporal to the fovea, which is designed to improve the coverage of the temporal macula. Macular ganglion cell complex thickness was defined as the combination of nerve fiber layer, ganglion cell layer, and inner plexiform layer. (33) Avanti software (Ver. 2017.0.0.16) derived a 6mm diameter ganglion cell complex thickness map centered 1 mm temporal to the fovea. Based on the map, overall, superior and inferior hemisphere average of the ganglion cell complex were obtained. Two special pattern analyses parameters were also obtained: a) the global loss volume (GLV), which measures all negative deviation values normalized by the overall map area, and, b) the focal loss volume (FLV), which measures the negative deviation values in areas of significant focal loss in the foveal region.[35]

Optic nerve head scans consisted of 13 concentric ring scans (1.3-4.9 mm diameter) and 12 radial line scans (3.4 mm in length) centered on the optic nerve head and automatically registered with the 3-dimensional scan to provide the disc margin information. The nerve fiber layer thickness

profile at 3.4 mm diameter was resampled on the nerve fiber layer map according to the detected optical center. The radial scans were segmented to calculate the cup-to-disc ratios and optic disc rim area. The optic nerve head scan was processed using Avanti software to delineate cup and disc boundaries. The horizontal cup-to-disc ratio is the ratio of the diameter of the cup portion with the total diameter of the optic disc in horizontal direction. The vertical cup-to-disc is the ratio in vertical direction. The cup-to-disc ratio of area is the ratio of cup area and disc areas. Scans were excluded if there was evidence of macular disease not related to glaucoma, ganglion cell complex signal strength index (SSI) below 39, and refractive error above –8.00 diopters.

In summary, the collected measurements using fourier domain optical coherence tomography included 1) the overall, superior and inferior hemisphere averages of the ganglion cell complex thickness map, 2) the overall, superior and inferior quadrants averages of the nerve fiber layer thickness profiles, 3) focal loss volume and global loss volume of ganglion cell complex thickness map.

The visual field device used was the Octopus 900 perimeter (Haag-Streit AG, Switzerland). Fields were excluded if there were false positives and negatives above 30%. Using the visual field mean defect and square root of loss variance, the Enhanced Glaucoma Staging System chart stages for each eye were determined. To increase statistical power eyes that were in Enhanced Glaucoma Staging System Stage 0, borderline, or 1 were grouped into what we refer to as a ‘low risk’ group and Stage 2 or higher were grouped into a ‘high risk’ group.

For the first experiment, a logistic binomial model of probability was used to create area under the receiver operating characteristic curves for predictor variables. Secondly, average

predictions from a boot-strap experiment were determined for each predictor variable. For each of the 500 iterations we estimate the logistic regression for each predictor using a random sample representing 80% of the dataset. Using the parameters from that estimation we predict the Enhanced Glaucoma Staging System category using the remaining 20% of the data and calculate the percentage of times the model correctly predicted the Enhanced Glaucoma Staging System category. We report the average percentage of times the model correctly predicted the Enhanced Glaucoma Staging System category over the 500 iterations. This experiment attempts to quantify how well each variable predicts Enhanced Glaucoma Staging System 'out-of-sample'.

For the third experiment all possible linear combinations of predictor variables were used to estimate the logistic regression to help determine the area under the curve (AUC) of a multivariate model.

In the final experiment a machine learning algorithm was used to select the best possible model containing linear and interactive terms. The machine learning algorithm provides a systematic method for adding and removing terms from a generalized linear model based on their statistical significance in explaining the response variable. The method begins with an initial linear model and then compares the explanatory power of incrementally larger and smaller models. The robustness of this model will be tested in two ways. First, one row will be dropped from the data set and the model parameters will be re-estimated using the remaining data. Then the new parameters and the dropped row of data will be used to predict the dropped row's Enhanced Glaucoma Staging System classification observation.

Results:

186 eyes from 97 patients including 44 males and 53 females who were diagnosed with glaucoma were included in the study. Race showed a highly Caucasian study population with only one individual being African American and one individual being Asian. The average age of all participants was 68.7 years and ranged from 38-87. Table 1 shows the number of eyes categorized into each Enhanced Glaucoma Staging System category. To increase statistical power the eyes from category 0 to 1 in the Enhanced Glaucoma Staging System grading are grouped and all eyes in category 3 or higher are grouped. Table 1 shows that there are 111 Enhanced Glaucoma Staging System observations in the low-risk category and 75 Enhanced Glaucoma Staging System observations in the high-risk category. The set of measurements included as predictors and their summary statistics are displayed in Table 2. The table indicates that these data are well behaved. None of the series contain outliers or dramatic skewness. Inferior ganglion cell complex does have fat tails relative to the normal distribution kurtosis, but the values far from the center are not biasing the mean or standard deviation. Table 3 contains the results of the logistic binomial model of probability of being in the high-risk Enhanced Glaucoma Staging System category as a function of each of the predictors individually. The first column of Table 3 labelled area under the curve shows the area under the receiver operating characteristic (ROC) curve for each logistic regression. For a perfect classifier, area under the curve = 1. For a classifier that randomly assigns observations to classes, area under the curve = 0.5. The specification using only focal loss volume produces the highest area under the curve as an individual predictor of being in the high-risk Enhanced Glaucoma Staging System group. The ROC for this regression is plotted in Figure 1. The average nerve fiber layer and superior nerve fiber layer have the next highest area under the curves for these individual regressions.

The second column of Table 3 contains the average percentage of correct predictions from the logistic regressions from the boot-strap experiment. For this experiment focal loss volume category and superior nerve fiber layer produce the highest expectations of correct prediction out-of-sample. Increasing the size of the estimation data set (decreasing the size of the hold-out sample) did not qualitatively change these results, nor did increasing the number of iterations.

Table 4 contains the estimation results of using all 4095 possible linear combinations of predictor variables to estimate the logistic regression. The model with the highest area under the curve of 0.825 utilizes focal loss volume, focal loss volume category, superior nerve fiber layer, and sex as predictors.

Table 5 contains the results from the machine learning algorithm that includes predictor variables and their interactions. The algorithm selects a model with 8 linear terms and 7 interactive terms shown in Table 5. The interactive terms represent the importance of each linear term conditional on the value of the term they are multiplied with. This specification of the model produces an area under the curve of 0.92 and a receiver operating characteristic depicted in Figure 2. During the first test of robustness of the model, which a row of data is dropped and new parameters are estimated using the remaining data to then be used to predict the dropped row's Enhanced Glaucoma Staging System classification observation, it was found that the model correctly predicts 81% of the dropped observations in the sample and produces and average area under the curve of 91.7%. The second test of robustness for which a 20% hold-out sample is used, an average of 80% correct predictions was found. If the parameter estimates form Table 5 are used instead of re-estimating the model, an average of 86% correct predictions for the model

specification are found. While by no means definitive, these results support the use of this model specification using measurements outside of our sample.

Discussion

Glaucoma is a complex disease and the amount of diagnostic information available to practitioners continues to increase with advancing technology. The glaucoma clinician, therefore, has a greater responsibility to not only differentiate glaucoma suspects and ocular hypertensives from true glaucomatous conversions, but also differentiating the severity of glaucoma damage in an eye.

Visual field testing has developed classifying systems to indicate the severity of glaucoma damage including Hodapp-Parrish-Anderson and Enhanced Glaucoma Staging System grading scales among others.[5,6] There have been efforts to create optical coherence tomography indexes to identify patients that are likely to convert from normal to glaucoma[34], as well as create consistent metrics to better classify disease severity.[36]

In this paper we have attempted to determine if looking more closely at the nerve fiber layer and ganglion cell complex optical coherence tomography parameters, specifically focal loss volume % and global loss volume %, can help predict the severity of glaucoma based on Enhanced Glaucoma Staging System grading system. When looking at individual predictors focal loss volume had the highest area under the curve and Inferior nerve fiber layer and average nerve fiber layer were a close second. Previous research has also highlighted the importance of inferior nerve fiber layer and focal loss volume while using optical coherence tomography parameters when investigating glaucoma.[29,36,37,38,39] Zhang and colleagues recognized focal loss volume to

be the most reliable single predictor of conversion of pre-perimetric glaucoma patients to perimetric glaucoma when looking at area under the receiver operating characteristics curve.[29] Their results also show that patients with an abnormal or borderline focal loss volume category had a 41% chance of converting to perimetric glaucoma by their 6 year follow up compared to just 10% of the patients with a normal focal loss volume.[29]

They also found most of the other nerve fiber layer and ganglion cell complex parameters to be important variables when analyzed individually. Our results also indicate that when using single predictors focal loss volume and inferior nerve fiber layer mildly outperform their other ganglion cell complex and nerve fiber layer counterparts. However, we found all the area under the curves to be similar for individual parameters with a range of 0.79 - 0.70, indicating that using a single predictor to try and predict the visual field may be too simplistic.

When using multivariate cox regression analysis, Zhang and colleagues found that visual field pattern standard deviation, inferior nerve fiber layer and focal loss volume combined to make the best model for conversion from normal to glaucoma.[37] Loewen and colleagues also found that in their multivariate logistic model to construct Glaucoma Structural Diagnostic Index that focal loss volume was one of the variables included along with overall ganglion cell complex and nerve fiber layer thickness and vertical cup-to-disc ratio.[34] Our best linear combination of variables also found focal loss volume along with focal loss volume category, superior nerve fiber layer, and sex made the best model to try and predict Enhanced Glaucoma Staging System category. Using multiple variables to try and predict Enhanced Glaucoma Staging System also improved the area under the curve compared to single predictors. This also agrees with several other studies which indicate that nerve fiber layer and ganglion cell complex components may

be complementary in diagnosing, classifying and tracking progression in glaucoma patients.[26,29,33,38] When we made the model more complex by using variables and their interactions as seen in Table 5, we were able to improve the area under the curve for predicting Enhanced Glaucoma Staging System grouping. This may indicate that it is feasible to create an optical coherence tomography index that could categorize severity of glaucoma which could correlate to the visual field severity as well.

One weakness of our study is that we only included one visual field and optical coherence tomography for each eye, this may be more of an issue for the visual field which can be prone to reproducibility issues. Also, we did not include cupping measurements from the optical coherence tomography data into our models, which could have improved our models especially since optical coherence tomography vertical cupping measurements was useful in creating the glaucoma structural diagnostic index.[34] In this study we combined Enhanced Glaucoma Staging System categories together to create two groups. With a larger data set it would be beneficial to see if keeping the standard Enhanced Glaucoma Staging System groupings increased the predictive value of the models or possibly make it worse. Loewen and colleagues used Hodapp-Parish-Anderson grading scale compared to normal subjects and had poor area under the curve results for borderline and grade 1 subjects compared to normal subjects even when using their index with multiple variables to predict visual severity.[34] It is reasonable to think that when trying to predict Enhanced Glaucoma Staging System categories that are similar, there will be increasing overlap of optical coherence parameter measurements between the two groups as well.

In conclusion, focal loss volume and global loss volume and other optical coherence tomography parameters may be useful to incorporate into a multivariate model that also takes interactions into account to help clinicians determine the severity of their patient's glaucoma.

References

1. Quigley H, Broman A. The Number of People with Glaucoma Worldwide in 2010 and 2020. Br J of Ophthalmol 2006;90:262-7.
2. National Institiute of Health. National Eye Institute. Projections for Glaucoma. Available at nei.nih.gov/eyedata/glaucoma#5. Accessed January 3, 2019.
3. Chauhan BC, Garway-Heath DF, Goñi FJ, et al. Practical Recommendations for Measuring Rates of Visual Field Change in Glaucoma. British J of Ophthalmol 2008;92:569-73.
4. Traynis I, De Moraes CG, Raza AS, et al. Prevalence and Nature of Early Glaucomatous Defects in the Central 10 of the Visual Field. JAMA Ophthalmol 2014;132:291-7.
5. Brusini P, Filacorda S. Enhanced Glaucoma Staging System (GSS 2) for Classifying Functional Damage in Glaucoma. J Glaucoma 2006;15:40-6.
6. Hodapp E, Parrish II R, Anderson D. Clinical Decisions in Glaucoma. St. Louis: Mosby-Year Book, Inc.; 1993.
7. Artes PH, O'Leary N, Hutchison DM, et al. Properties of the statpac visual field index. Invest Ophthalmol Vis Sci 2011;52:4030-8.
8. Medeiros FA, Weinreb RN, Moore G, et al. Integrating Event-and Trend-based Analyses to Improve Detection of Glaucomatous Visual Field Progression. Ophthalmol 2012;119:458-67.

9. Wilsey LJ, Fortune B. Electroretinography in Glaucoma Diagnosis. Cur Opin Ophthalmol 2016;27:118.
10. Bode SF, Jehle T, Bach M. Pattern Electroretinogram in Glaucoma Suspects: New Findings from a Longitudinal Study. Invest Ophthalmol Vis Sci 2011;52:4300–6.
11. Niyadurupola N, Luu CD, Nguyen DQ, et al. Intraocular Pressure Lowering is Associated with an Increase in the Photopic Negative Response (PhNR) Amplitude in Glaucoma and Ocular Hypertensive Eyes. Invest Ophthalmol Vis Sci 2013;54:1913–19.
12. Spaeth G, Reddy S. Imaging of the Optic Disk in Caring for Patients with Glaucoma: Ophthalmoscopy and Photography Remain the Gold Standard. Surv of Ophthalmol 2014;59:454-8.
13. Jampel H, Friedman D, Quigley H. Agreement Among Glaucoma Specialists in Assessing Progressive Disc Changes from Photographs in Open-angle Glaucoma Patients. Am J Ophthalmol 2009;147:39–44.
14. Azuara-Blanco A, Katz L, Spaeth G, et al. Clinical agreement among glaucoma experts in the detection of glaucomatous changes of the optic disk using simultaneous stereoscopic photographs. Am J Ophthalmol 2003;136:949–50.
15. Cymbor M, Lear L, Mastrine M. Concordance of Flicker Comparison Versus Side-by-side Comparison in Glaucoma. Optom J Ameri Optom Assoc 2009;80:437-41.
16. Zangwill L, Jain S, Dirkes K, et al. Confocal Scanning Laser Ophthalmoscopy Ancillary Study to the Ocular Hypertension Treatment Study. The Rate of Structural Change: the Confocal Scanning Laser Ophthalmoscopy Ancillary Study to the Ocular Hypertension Treatment Study. Am J Ophthalmol 2013;155:971-82.

17. Mohammadi K, Bowd C, Weinreb RN, et al. Retinal Nerve Fiber Layer Thickness Measurements with Scanning Laser Polarimetry Predict Glaucomatous Visual Field Loss. Am J of Ophthalmol 2004;138:592-601.
18. Vizzeri G, Bowd C, Medeiros F, et al. Effect of Improper Scan Alignment on Retinal Nerve Fiber Layer Thickness Measurements using Stratus Optical Coherence Tomograph. J Glaucoma 2008;17:341–9.
19. Wojtkowski M, Srinivasan V, Ko T, et al. Ultrahigh-Resolution, High-Speed, Fourier Domain Optical Coherence Tomography and Methods for Dispersion Compensation. Opt Exp 2004;12:2404–22.
20. González-García A, Vizzeri G, Bowd C, et al. Reproducibility of Rtvue Retinal Nerve Fiber Layer Thickness and Optic Disc Measurements and Agreement with Stratus Optical Coherence Tomography Measurements. Am J Ophthalmol 2009;147:1067–74.
21. Lalezary M, Medeiros FA, Weinreb RN, et al. Baseline Optical Coherence Tomography Predicts the Development of Glaucomatous Change in Glaucoma Suspects. American J Ophthalmol 2006;142:576-82.
22. Hood DC, Slobodnick A, Raza AS, et al. Early Glaucoma Involves Both Deep Local, and Shallow Widespread, Retinal Nerve Fiber Damage of the Macular Region. Invest Ophthalmol Vis Sci 2014;55:632-49.
23. Na J, Lee K, Lee J, et al. Detection of Macular Ganglion Cell Loss in Preperimetric Glaucoma Patients With Localized Retinal Nerve Fiber Defects by Spectral Domain Optical Coherence Tomography. Clin Exp Ophthalmol 2013;41:870-80.

24. Ohkubo S, Higashide T, Udagawa S, et al. Focal Relationship Between Structure and Function Within the Central 10 Degrees in Glaucoma Focal Relationship Between Structure and Function. Invest Opthalmol Vis Sci 2013;55:5269-77.
25. Kita Y, Kita R, Takeyama A, et. Ability of Optical Coherence Tomography–determined Ganglion Cell Complex Thickness to Total Retinal Thickness Ratio to Diagnose Glaucoma. J Glaucoma 2013 1;22:757-62.
26. Naghizadeh F, Garas A, Vargha P, et al. Detection of Early Glaucomatous Progression with Different Parameters of the Rtvue Optical Coherence Tomograph. J Glaucoma 2014;23(4):195-8.
27. Hood DC, Raza AS, de Moraes CG, et al. Glaucomatous Damage of the Macula. Prog Ret Eye Res 2013;32:1-21.
28. Kuang TM, Zhang C, Zangwill LM, et al. Estimating Lead Time Gained by Optical Coherence Tomography in Detecting Glaucoma Before Development of Visual Field Defects. Ophthalmol 2015;122:2002-9.
29. Zhang X, Dastiridou A, Francis BA, et al. Comparison of Glaucoma Progression Detection by Optical Coherence Tomography and Visual Field. Am J Ophthalmol 2017;184:63-74.
30. Holló G, Zhou Q. Evaluation of Retinal Nerve Fiber Layer Thickness and Ganglion Cell Complex Progression Rates in Healthy, Ocular Hypertensive, and Glaucoma Eyes With The Avanti Rtvue-XR Optical Coherence Tomograph Based On 5-Year Follow-Up. J Glaucoma 2016;25.

31. Lin C, Mak H, Yu M, Leung CK. Trend-Based Progression Analysis for Examination of the Topography of Rates of Retinal Nerve Fiber Layer Thinning in Glaucoma. JAMA Ophthalmol 2017;135:189-95.
32. Hood DC, De Cuir N, Blumberg DM, et al. A Single Wide-Field OCT Protocol Can Provide Compelling Information for the Diagnosis of Early Glaucoma. Trans Vis Sci Tech 2016;5
33. Tan O, Chopra V, Lu AT, et al. Detection of Macular Ganglion Cell Loss in Glaucoma by Fourier-Domain Optical Coherence Tomography. Ophthalmol 2009;116:2305-14.
34. Loewen NA, Zhang X, Tan O, et al. Combining Measurements from Three Anatomical Areas for Glaucoma Diagnosis Using Fourier-Domain Optical Coherence Tomography. Br J Ophthalmol 2015;99:1224-9.
35. Sehi M, Goharian I, Konduru R, et al. Retinal Blood Flow in Glaucomatous Eyes with Single-Hemifield Damage. Ophthalmol 2014;121:750-8.
36. Zhang X, Loewen N, Tan O, et al. Predicting Development of Glaucomatous Visual Field Conversion Using Baseline Fourier-Domain Optical Coherence Tomography. Am J Ophthalmol 2016;163:29-37.
37. Kim NR, Lee ES, Seong GJ, et al. Structure–Function Relationship and Diagnostic Value of Macular Ganglion Cell Complex Measurement Using Fourier-Domain OCT in Glaucoma. Invest Opthalmol Vis Sci 2010;51:4646.
38. Larrosa JM, Moreno-Montañés J, Martinez-de-la-Casa JM, et al. A Diagnostic Calculator for Detecting Glaucoma on the Basis of Retinal Nerve Fiber Layer, Optic Disc, and Retinal Ganglion Cell Analysis by Optical Coherence Tomography. Invest Ophthalmol Vis Sci 2015;56:6788-95.

39. Medeiros FA, Zangwill LM, Alencar LM, et al. Detection of Glaucoma Progression with Stratus OCT Retinal Nerve Fiber Layer, Optic Nerve Head, and Macular Thickness Measurements. Invest Opthalmol Vis Sci 2009;50:5741-8.

Figure 1: Example of Avanti nerve fiber layer and ganglion cell complex report

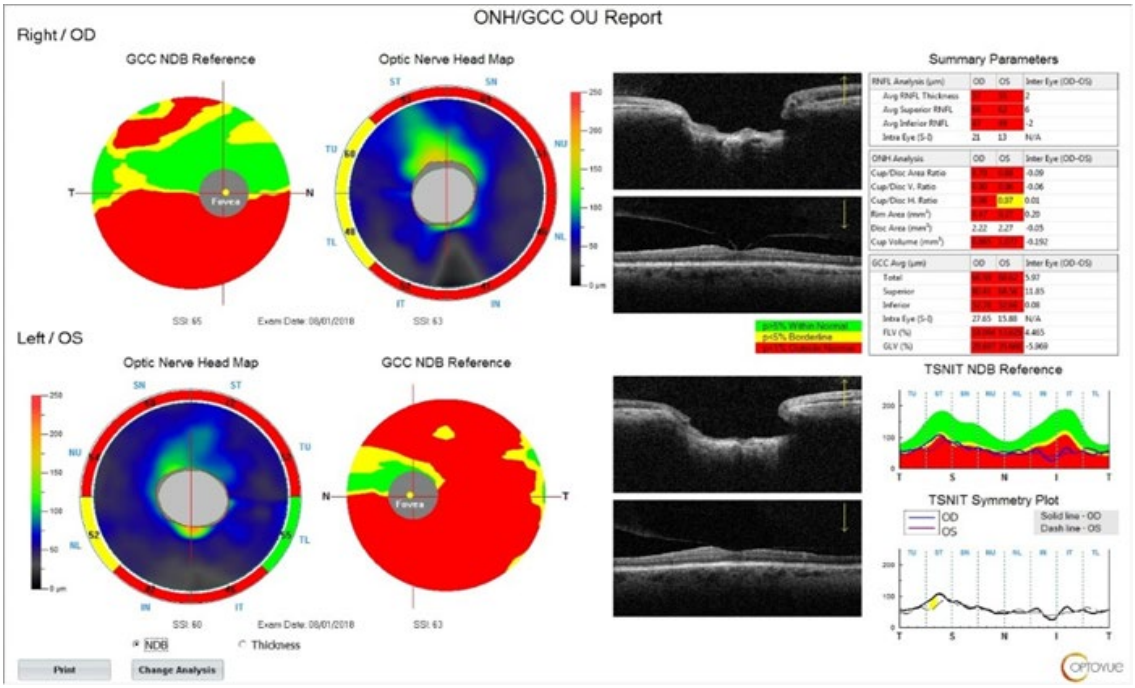

Figure 2: ROC for FLV

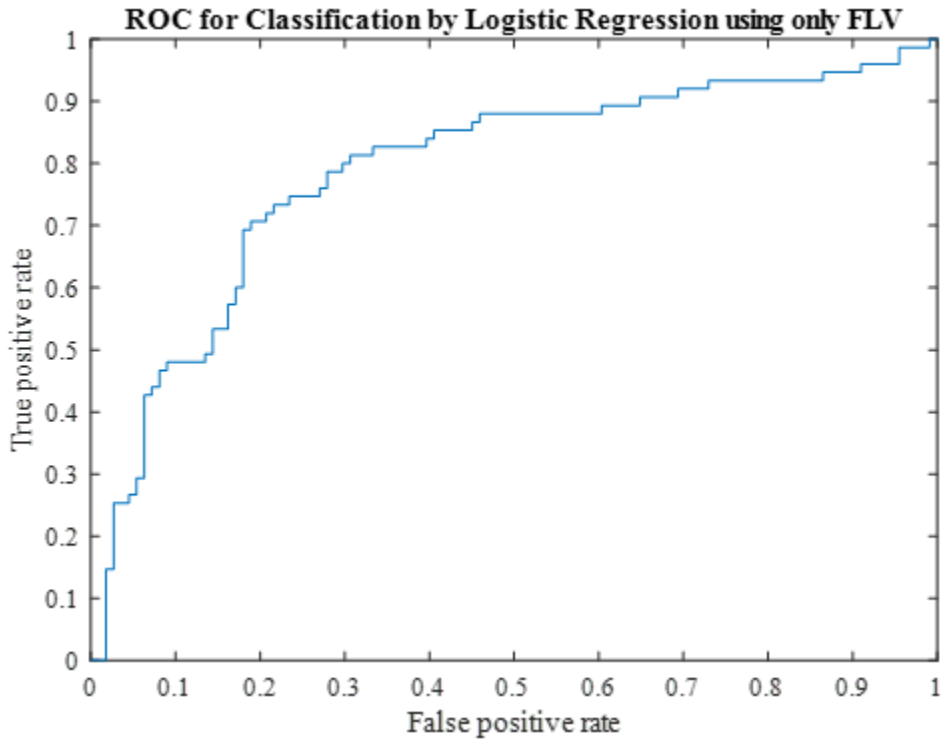

This figure contains the receiver operating characteristic (ROC) curve for the binomial logistic regression of Enhanced Glaucoma Staging System (GSS2) on Focal Loss Volume (FLV).

Figure 3: ROC for Interactive Specification

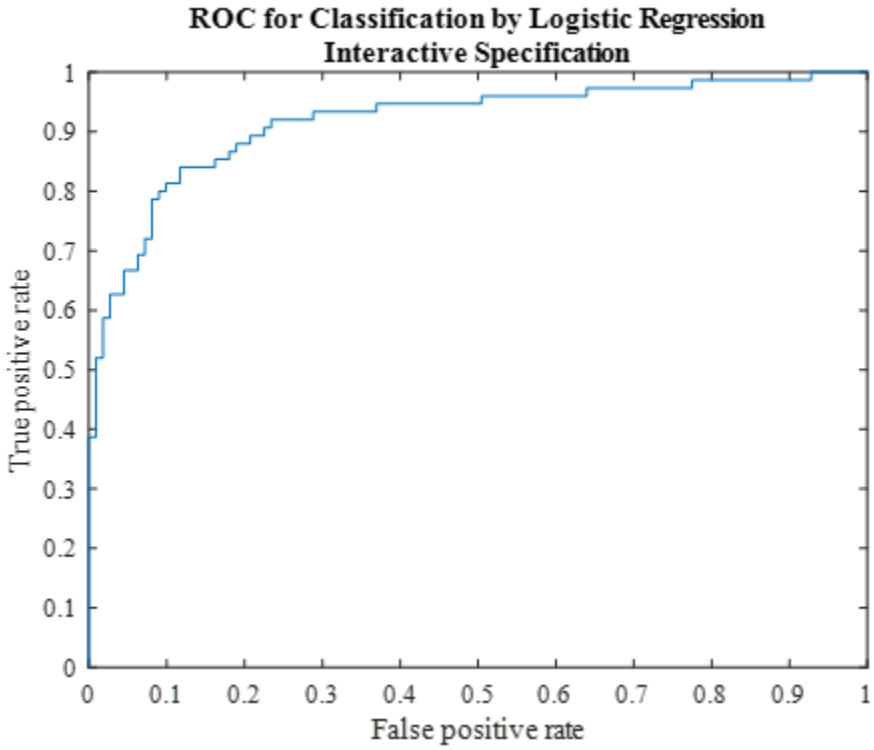

This figure contains the receiver operating characteristic (ROC) curve for the binomial logistic regression of GSS2 for the specification chosen by the machine learning algorithm.

Table 1: GSS2 Groupings

This table contains the size of the two groupings of Enhanced Glaucoma Staging System (GSS2). Stages 0 to 1 are in Group 1 while the remaining categories of GSS2 are placed in group 2.

GSS2	Low Risk	High Risk
0	52	
0.5	21	
1	38	
2		39
3		20
4		15
5		1
N	111	75

Table 2: Summary Statistics

This table contains summary statistics for the set of 12 measurements used as predictor variables. Our sample contains 186 observations. Std. Dev. is the standard deviation. Q25 and Q75 are the observations falling at the 25th and 75th percentiles. Note that FLV Category and GLV Category are categorical variables with values of 1, 2, or 3. Sex is a categorical variable with a value of 1 for Male and 2 for Female. GCC = Ganglion Cell Complex, FLV = Focal Loss Volume, GLV = Global Loss Volume, NFL = Nerve Fiber Layer

	Total GCC	Superior GCC	Inferior GCC	FLV	FLV Category	GLV	GLV Category	Average NFL	Superior NFL	Inferior NFL	Sex	Age
Mean	80.15	82.05	77.88	4.60	2.02	15.98	2.27	78.19	81.39	75.05	1.54	69.34
Median	81.00	82.00	78.00	3.31	2.00	14.76	3.00	78.00	81.00	75.00	2.00	70.00
Std. Dev.	10.35	10.27	13.14	4.27	0.93	9.51	0.82	11.99	12.66	13.29	0.50	8.93
Skewness	0.07	-0.14	-0.63	0.87	-0.04	0.26	-0.54	0.13	0.03	0.21	-0.17	-0.60
Kurtosis	2.46	2.53	6.00	2.86	1.16	2.25	1.70	2.52	2.49	2.53	1.03	3.78
Q25	72.00	75.00	68.00	0.84	1.00	9.51	2.00	69.00	72.00	65.00	1.00	64.00
Q75	87.00	90.00	86.00	7.75	3.00	23.92	3.00	87.00	91.00	85.00	2.00	75.00

Table 3: Individual Predictors

The first column labelled AUC contains area under the receiver operating characteristic (ROC) curve for a logistic regression where the response is the GSS2 grouping for low-risk and high-risk and the design matrix consists of each predictor individually. The second column contains the average value of the correctly predicted 500 bootstrap samples described in the text. GCC = Ganglion Cell Complex, FLV = Focal Loss Volume , GLV = Global Loss Volume, NFL = Nerve Fiber Layer

	AUC	Expected % Predicted Correctly
Total GCC	0.75	0.72
Superior GCC	0.70	0.69
Inferior GCC	0.75	0.73
FLV	**0.79**	0.72
FLV Category	0.76	**0.75**
GLV	0.75	0.72
GLV Category	0.70	0.68
Average NFL	**0.78**	**0.74**
Superior NFL	0.74	0.73
Inferior NFL	**0.78**	0.72
Sex	0.52	0.59
Age	0.51	0.60

Table 4: Best linear combination of variables

This table contains the estimation results of a binomial logistic regression where the response is the Enhanced Glaucoma Staging System (GSS2) grouping for low-risk and high-risk and the design matrix consists of the predictors Focal Loss Volume (FLV), FLV Category, Inferior NFL, and Sex. FLV = Focal Loss Volume, AUC = Area Under the Receiver Operating Characteristic Curve

	Estimate	*t*-Stat	*P*-Value
(Intercept)	3.40	2.10	0.036
FLV	0.19	2.18	0.029
FLV Category	0.36	0.96	0.34
Superior NFL	-0.06	-3.70	< .0001
Sex	-0.38	-0.99	0.32
N =	186		
Degrees of Freedom	181		
c^2 statistic vs. constant model		c^2 = 67.6	*P* < .0001
AUC =	**0.825**		

Table 5: Interaction Model

The table contains the results of the binomial logistic regression where the response is the GSS2 grouping for low- and high-risk for the model selected by the machine learning algorithm described in the text. GCC = Ganglion Cell Complex, FLV = Focal Loss Volume, NFL = Nerve Fiber Layer, AUC = Area Under the Receiver Operating Characteristic Curve

	Estimate	*t*-Stat	*P*-Value
(Intercept)	46.220	1.920	.055
Inferior GCC	0.374	3.187	.001
FLV	-1.026	-2.286	.02
FLV Category	9.924	3.089	.002
Average NFL	-0.564	-0.916	.36
Superior NFL	-1.353	-3.192	.001
Inferior NFL	0.854	1.798	.07
Sex	19.906	2.999	.003
Age	-1.070	-3.852	< .0001
Inferior GCC*Sex	-0.183	-2.781	.005
FLV*Age	0.021	2.933	.003
FLV Category*Superior NFL	-0.070	-2.145	.03
FLV Category*Sex	-2.839	-3.292	.001
Average NFL*Superior NFL	0.018	3.439	.001
Superior NFL*Inferior NFL	-0.017	-3.012	.003
Superior NFL*Age	0.012	3.589	< .0001
N =	186		
Degrees of Freedom =	170		
c^2 statistic vs. constant model		c^2 = 121	*P* < .0001
AUC =	**0.92**		